MEDICAL SCIENCE MONITOR

CLINICAL RESEARCH

e-ISSN 1643-3750
© Med Sci Monit, 2019; 25: 61-70
DOI: 10.12659/MSM.911120

Received: 2018.05.14
Accepted: 2018.07.31
Published: 2019.01.03

Selenium-Rich Diet Induces Myocardial Structural and Functional Abnormalities by Activating Caspase-9 and Caspase-3 in Gpx-1P198L-Overexpression Transgenic Mice

Authors' Contribution:
Study Design A
Data Collection B
Statistical Analysis C
Data Interpretation D
Manuscript Preparation E
Literature Search F
Funds Collection G

BCDEF 1,2 Suqin Wang*
BCDF 3 Xiting Nong*
ABCDEFG 4 Guang Yang

1 Department of Cardiology, Fuwai Central China Cardiovascular Hospital, Zhengzhou, Henan, P.R. China
2 Department of Cardiology, People's Hospital of Henan Province, Zhengzhou, Henan, P.R. China
3 Department of Endocrinology, Xi'an Central Hospital, Xi'an, Shaanxi, P.R. China
4 Department of Cardiology, Shaanxi Provincial People's Hospital, Xi'an, Shaanxi, P.R. China

* Suqin Wang and Xiting Nong contributed equally to this work

Corresponding Author: Guang Yang, e-mail: yanggshx@hainan.net

Source of support: This study was supported by the General Program of the National Natural Science Foundation of China (Grant No. 30972557)

Background: Selenium (Se) deficiency and supplementation result in multiple effects. GPx-1 (Pro198Leu) polymorphism is associated with Se deficiency. This study aimed to observe associations between Se-deficiency/supplement and GPx-1-198Leu overexpression in myocardial injuries.

Material/Methods: GPx-1P198L transgenic (Tg) mice and non-transgenic wild-type (WT) littermates were divided into Control (CON, 0.1–0.2 mg/kg), Se-deficiency (SD, <0.02 mg/kg), and Se-supplement (SS, 0.4 mg/kg) groups. Cardiac functions were observed with animal M-mode echocardiography. Se level was measured using 2,3-diamino Kenai fluorospectrophotometry. Total cardiac GPx activity was also measured. Myocardial histopathology was determined with HE and Masson's trichrome staining. Caspase-9 and caspase-3 were measured with Western blot analysis.

Results: In WT Se-deficient mice, cardiac GPx activity was significantly decreased, and was not elevated by overexpression of GPx-1-198Leu gene. Increased GPx activity was observed in WT Se-supplemented mice and Tg Se-supplemented mice (much more). Se deficiency as well as supplementation resulted in cardiac systolic dysfunction, which was not affected by GPx-1-198Leu gene. Se deficiency led to myocardial fibrosis and pathological changes accompanied by increased activation of caspase-9 and caspase-3. Se supplementation significantly reduced pathological changes, as well as caspase-9 and caspase-3 levels in the presence of increased myocardial fibrosis. In Se-deficient mice, GPx-1-198Leu overexpression did not significantly decrease myocardial pathological injuries and fibrosis. In Se-supplemented Tg mice, myocardial fibrosis and caspase-9 level were increased, although pathological injuries and caspase-3 were similar to that in Se-supplemented WT mice.

Conclusions: Se deficiency as well as supplementation induced myocardial structural and functional abnormalities through activation of caspase-9 and caspase-3 in GPx-1P198L overexpression transgenic mice.

MeSH Keywords: Apoptosis • Endomyocardial Fibrosis • Mice, Transgenic • Selenium

Full-text PDF: https://www.medscimonit.com/abstract/index/idArt/911120

Indexed in: [Current Contents/Clinical Medicine] [SCI Expanded] [ISI Alerting System] [ISI Journals Master List] [Index Medicus/MEDLINE] [EMBASE/Excerpta Medica] [Chemical Abstracts/CAS]

Background

Selenium (Se) is well established as an essential trace element that plays critical roles in chemo-protection against oxidative stress, but high concentrations of Se induce toxic and oxidative effects [1–3]. In fact, different levels of Se have different effects. It has been reported that Se at higher concentrations decreases cell proliferation and causes apoptosis in A20 and NB4 cells [4,5]. Dietary Se deficiency is considered to be a causative factor of the endemic cardiomyopathy prevalent in China, termed Keshan disease (KD) [6]. Lower blood Se levels are observed in patients with reduced left ventricular systolic heart failure [7,8]. Metes-Kosik et al. found that both Se deficiency and modest Se supplementation resulted in a similar phenotype of abnormal myocardial matrix remodeling and dysfunction in the normal heart [9]. Therefore, appropriate amounts of Se are required for optimal body health.

Mitochondria play an important role in apoptosis under various proapoptotic conditions. If mitochondria are exposed to proapoptotic signals, such as reactive oxygen species (ROS), mitochondrial cytochrome c is released into cytosol, binds to Apaf-1, and then participates in caspase-9 activation. The activated capase-9 consequently activates caspase-3, which in turn activates a caspase-activated DNase and leads to DNA degradation, a hallmark of apoptosis [10]. However, ROS production is part of the normal cellular metabolism and may function as signaling molecules necessary for cell growth and survival [11,12]. Accumulating evidence has indicated that ROS such as superoxide anion and hydrogen peroxide may be related to cell death and play an important role in a variety of oxidative stress-induced disorders [13–15]. GPx-1 an crucial antioxidant because it is located in both the cytosol and the mitochondrial matrix and it can reduce lipid peroxides and hydrogen peroxide into corresponding alcohols and water. As a Se-dependent enzyme, Gpx-1 activity decreases dramatically in Se deficiency and increases during Se supplementation. GPx-1 activity is also associated with GPx-1 (Pro198Leu) polymorphism and Se deficiency [16]. The Leu allele was found to be less responsive to increased Se levels than the Pro allele [17]. Moreover, a variety of evidence has indicated that the GPx-1 (Pro198Leu) polymorphism is associated with many oxidative stress-related diseases, such as endemic cardiomyopathy, cancers, and diabetic complications [16,18,19].

Overexpression of GPx-1 can ameliorate myocardial remodeling and failure in diabetic mice, as well as in mice with myocardial infarction, via prevention of oxidative stress [20,21]. However, growing evidence has indicated that increased GPx-1 activity might be related to hyperglycemia, hyperinsulinemia, insulin resistance, and obesity observed in Gpx1-overexpressing mice [22,23]. Thus, the aim of the present study was to investigate the effects of different Se diets on cardiac structure and function, as well as activation of caspase-9 and -3, in mice overexpressing the human GPx-1-198leu gene.

Material and Methods

Transgenic mice

Our study was approved by the Institutional Animal Research Committee and conformed to the animal care guidelines of the Medical College of Xi'an Jiaotong University. Human mutated GPx-1-198Leu mRNA was recombined according to NCBI reference sequence NM_000581.2 and then inserted downstream of the human cytomegalovirus (CMV) immediate early promoter of plasmid pEGFP-N3. Part of GFP sequence was cut so that hGPx-1-198Leu could successfully and effectively be expressed. Identification of the transgenic vector was performed by PCR and sequencing. After linearization with AseI and AflII, the transgenic piece including hGPx-1-198Leu, CMV promoter, and SV40 polyA was microinjected into fertilized eggs derived from C57BL/6J mice. The GPx-1-198Leu-overexpressing mice were designated as GPx-1P198L transgenic mice. The genotype of GPx-1P198L transgenic mice was detected by PCR, and hGPx-1-198Leu expression levels in the hearts of transgenic mice was determined by Western blot analysis. Four lines of transgenic mice carrying extra copies of the human GPx-1-198Leu gene were generated.

Diets and treatments

Twenty-seven 3-week old weanling transgenic mice were used and were randomly divided into 3 groups. Nine mice within each group (♀ 4, ♂ 5) were fed a Se-deficient diet (SD, <0.02 mg Se/kg) [24] with all the other nutrients at the standard level. The second group (♀ 4, ♂ 5) was fed a Se-supplemented diet (SS, the SD diet supplemented with sodium selenite 0.4 mg Se/kg) [24]. The last group (♀ 4, ♂ 5) was fed a standard diet as a control (CON, with a content of 0.1–0.2 mg Se/kg). Twenty-seven weaning non-transgenic wild-type C57BL/6J littermates (♀ 4, ♂ 5 for each group) were treated the same as transgenic mice. All animals were individually housed in an SPF animal room with a constant temperature (22°C) and a 12: 12 h light-to-dark cycle and were given free access to distilled water and chow for 12 weeks. The standard diet was supplied by the Animal Experimental Center of Xi'an Jiaotong University and the SD and SS diets were purchased from Trophic Animal Feed Hightech Co. (Jiangsu, China) according to the AIN-93M formula [25,26].

Echocardiographic measurements of cardiac function

For measurements of cardiac function, echocardiographic studies were performed in 6 anesthetized mice in each group

Indexed in: [Current Contents/Clinical Medicine] [SCI Expanded] [ISI Alerting System] [ISI Journals Master List] [Index Medicus/MEDLINE] [EMBASE/Excerpta Medica] [Chemical Abstracts/CAS]

with isoflurane 2–2.5 ml/min and spontaneous respiration. Parameters of interventricular septum wall thickness (IVSs, IVSd), left ventricular posterior wall thickness (LVPWs, LVPWd), left ventricular end-systolic diameter (LVESD), left ventricular end-diastolic diameter (LVEDD), left ventricular end-systolic volume (LVESV), left ventricular end-diastolic volume (LVEDV), ejection fraction (EF), and fractional shortening (FS) were evaluated using a M-mode echocardiography (Vevo2100, Canada).

Serum Se

After detection of cardiac function, whole blood from the 6 animals per group was collected for the determination of serum Se, which was analyzed by a flameless atomic absorption spectrophotometry method using a Z-5000 spectrophotometer (Hitachi, Japan) with a Se cathode lamp (resonance line, 196.0 nm, Photron, Australia).

Sample collection

After the above studies, the hearts were excised and the LV was immediately fixed in 10% formalin solution for 24 h, then embedded in paraffin. We cut 4-μm sections and stained them with hematoxylin and eosin for myocardial histopathology observation, as well as staining with Masson's trichrome for collagen distribution determination. The remaining 3 mouse hearts were also excised, cut into 2 parts each, and stored at –80°C for protein extraction.

Myocardial GPx activity

From the samples stored at –80°C, one part was homogenized in physiological saline on ice, centrifuged at 3000 rpm for 15 min, and supernatant was recollected. Myocardial GPx activity was spectrophotometrically measured using a cellular glutathione peroxidase activity assay kit (Nanjing Jiancheng, China), according to the manufacturer's instructions.

Western blot analysis of caspase-9 and -3 levels

Western blot procedures followed previously described methods [27]. From the other part of the samples stored at –80°C, cytosol protein was also extracted using RIPA lysis (1% PMSF) on ice and centrifuged at 14 000 r/min for 20 min. After denaturation, the supernatant was stored at –20°C and set aside for analysis of apoptosis-related genes caspase-9 and -3. Rabbit anti-caspase-9 and rabbit anti-caspase-3 were diluted in PBST (1: 100 dilution, Wuhan Boster, China). GAPDH was detected as control (mouse anti-GAPDH, 1: 1000 dilution, Shanghai Abgent, China). Secondary antibodies used were HRP-conjugated goat anti-rabbit IgG (1: 5000 dilution, Xi'an Jingcai, China) and HRP-conjugated goat anti-mouse IgG (1: 4000 dilution, Xi'an Jingcai, China).

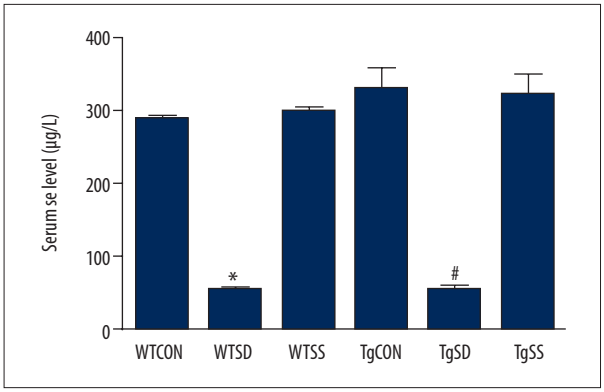

Figure 1. Effect of different diets on serum Se level in each group. (**A**) Effect on serum Se level. (**B**) Effect on cardiac GPx activity. WTCON – wild-type control mice, WTSD – wild-type Se-deficient mice, WTSS – wild-type Se-supplemented mice, TgCON – transgenic control mice, TgSD – transgenic Se-deficient mice, TgSS – transgenic Se-supplemented mice. * $p<0.0001$ *vs.* WTCON, WTSS, # $p<0.0001$ *vs.* TgCON, TgSS.

Statistical analysis

All of the data were analyzed using SPSS software 22.0 (SPSS Inc., Chicago, IL, USA). The quantitative data were recorded as mean ± standard deviation and analyzed using the *t* test for comparisons between 2 groups. Tukey's post hoc test was used to validate ANOVA for comparing measurement data between groups. All the data were obtained from at least 6 independent tests or experiments. Statistical significance was defined as $p<0.05$.

Results

Serum Se concentrations and myocardial GPx activity

In the WT mice, serum Se level was significantly decreased in the SD group compared with the CON group (Figure 1, $p<0.0001$), and although the Se level in the SS group was higher, it was not significantly elevated compared with the CON group. Serum Se levels in the Tg groups were the same as in the WT groups. Cardiac GPx activity in the SD group was significantly lower compared with the CON group (Figure 2, $p<0.05$) not only in WT mice, but also in Tg mice. GPx activity in the SS group was significantly increased compared with the CON group (Figure 2, $p<0.05$) in WT mice as well as in Tg mice. GPx activity was not significantly different between WTCON and TgCON (Figure 2, $p=0.206$) or between WTSD and TgSD (Figure 2, $p=0.625$), but GPx activity in TgSS was significantly higher than that in the WTSS group (Figure 2, $p<0.0001$).

Indexed in: [Current Contents/Clinical Medicine] [SCI Expanded] [ISI Alerting System] [ISI Journals Master List] [Index Medicus/MEDLINE] [EMBASE/Excerpta Medica] [Chemical Abstracts/CAS]

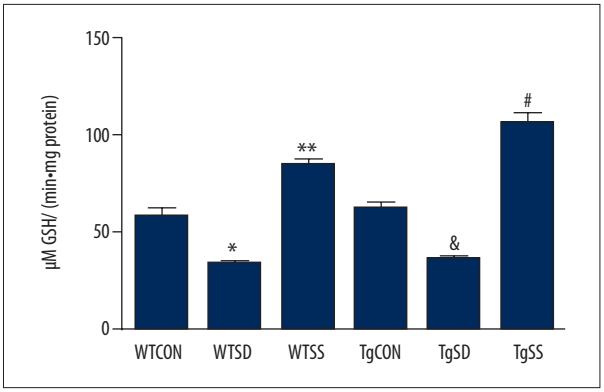

Figure 2. Effect of different diets on cardiac GPx activity in each group. WTCON – wild-type control mice, WTSD – wild-type Se-deficient mice, WTSS – wild-type Se-supplemented mice, TgCON – transgenic control mice, TgSD – transgenic Se-deficient mice, TgSS – transgenic Se-supplemented mice. * $p<0.05$ *vs.* WTCON, ** $p<0.05$ *vs.* WTCON, WTSD; & $p<0.05$ *vs.* TgCON, # $p<0.05$ *p*TgCON, TgSD, WTSS.

Echocardiographic measurements

The echocardiographic data of mice are shown in Table 1 and Figure 3. IVSs in WTSD was significantly decreased over that in WTCON ($p=0.009$). IVSs in TgSD and TgSS tended to decrease ($p=0.049$, 0.055). LVPWs and LVPWd in WTSD and TgSD were thinner but with no significant difference from those in the respective control group. LVESD in WTSD was significantly increased over that in WTCON ($p<0.05$). LVESD and LVEDD in TgSD was significantly increased over that in TgCON ($p<0.05$). LVEDV and LVESV in WTSD and TgSD were remarkably larger than those in the respective WTCON and TgCON ($p<0.05$). Moreover, LVESV in TgSS was also significantly increased over that in TgCON ($p<0.05$). EF and FS in SD and SS groups were significantly decreased over those in the CON group in WT mice as well as in Tg mice.

Myocardial histopathology

In the WT mice in the SD group, myocytes were small and arranged in a wave-like pattern, more inflammatory cells were found, and gaps between myocytes were widened compared with the CON group. In the SS group, myocytes were larger and arranged in a wave-like pattern, more inflammatory cells were observed, and gaps between myocytes were narrowed compared with the CON group. In the Tg mice, the pathological changes in SD and SS groups were similar to the respective WTSD and WTSS groups (Figure 4).

Myocardial fibrosis

Masson's trichrome staining showed that myocardial fibrosis in WTSD and WTSS groups were significantly increased compared with the WTCON group (Figure 5, $p<0.05$), and myocardial

Table 1. Parameters of LV from mice in each group (n=6, mean ±SD).

	WT			Tg		
	CON	SD	SS	CON	SD	SS
IVSd (mm)	0.98±0.09	0.96±0.1	0.95±0.25	1±0.08	1.06±0.15	0.95±0.15
IVSs (MM)	1.5±0.15	1.13±0.18	1.49±0.18	1.45±0.12	1.38±0.16	1.24±0.08
LVPWd (mm)	1.19±0.2	0.87±0.44	1±0.52	1±0.52	0.85±0.5	1.9±0.59
LVPWs (mm)	1.76±0.16	1.18±0.06	1.49±0.15	1.36±0.43	1.13±0.37	2.23±0.67
LVEDD (mm)	4.21±0.3	4.79±0.08	4.46±0.69	3.85±0.56	5.33±0.71	4.62±0.9
LVESD (MM)	3.03±0.28	4.34±0.01	3.61±0.53	2.9±0.55	4.8±0.75	3.9±0.89
LVEDV (μl)	59.4±11.22	127.13±13.96	92.57±33.61	61.94±22.74	139.44±42.16	102.12±43.02
LVESV (μl)	27.48±15.84	84.77±2.58	55.98±19.32	26.9±9.8	110.05±38.8	69.18±33.75
EF (%)	53.91±1.56	20.71±3	39.36±3.42	56.59±1.65	21.94±4.31	34.04±6.71
FS (%)	28.13±1.59	9.43±1.46	19±1.93	24.99±3.98	10.12±2	16.17±3.32

LV – left ventricle; IVSd – interventricular septum diastolic thickness. IVSs – interventricular septum systolic thickness; PWd – posterior diastolic wall thickness; PWs – posterior systolic wall thickness; ESD – end-systolic diameter; EDD – end-diastolic diameter; ESV – end-systolic volume; EDV – end-diastolic volume; EF – ejection fraction; FS – fractional shortening; WTCON – wild-type control mice; WTSD – wild-type Se-deficient mice; WTSS – wild-type Se-supplemented mice; TgCON – transgenic control mice; TgSD – transgenic Se-deficient mice; TgSS – transgenic Se-supplemented mice. * $p<0.05$ *vs.* WTCON, WTSS; # $p<0.05$ *vs.* WTSS, TgCON, TgSD; & $p<0.05$ *vs.* WTCON; ## $p<0.05$ *vs.* TgCON.

Indexed in: [Current Contents/Clinical Medicine] [SCI Expanded] [ISI Alerting System] [ISI Journals Master List] [Index Medicus/MEDLINE] [EMBASE/Excerpta Medica] [Chemical Abstracts/CAS]

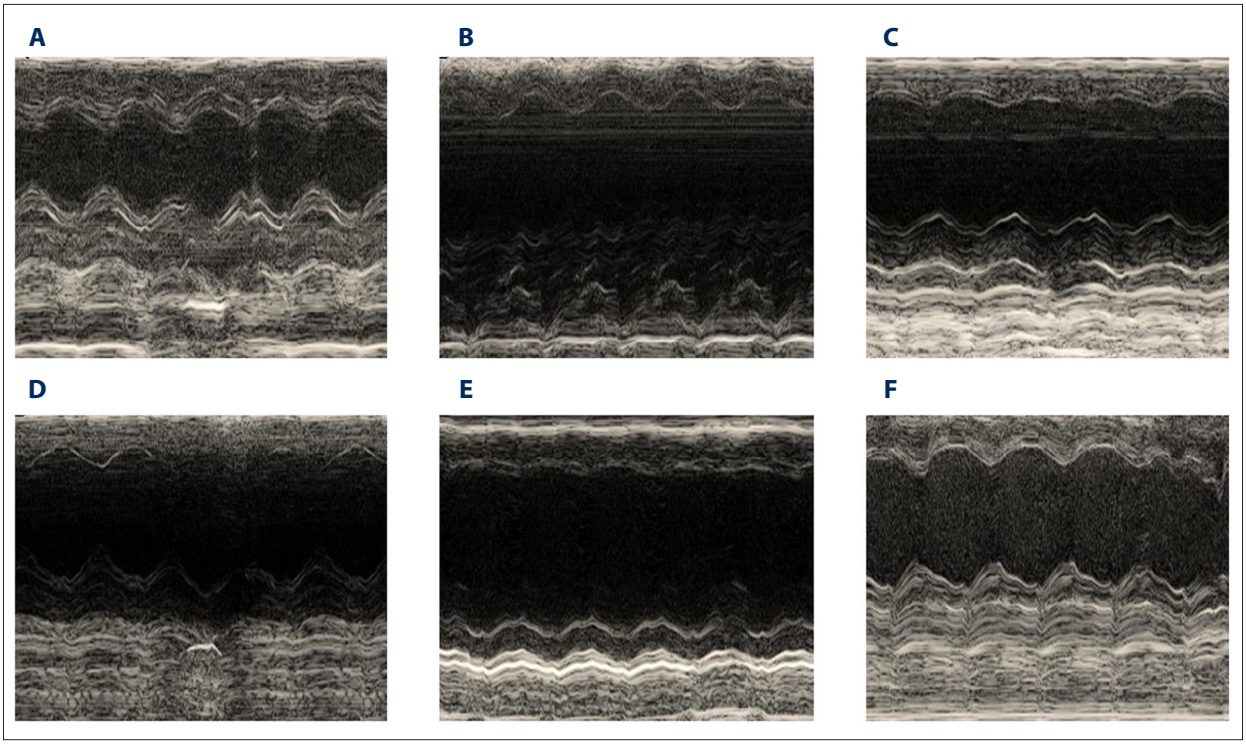

Figure 3. M-mode echocardiography of mice in each group. (**A**) Wild-type control mice. (**B**) Wild-type Se-deficient mice. (**C**) Wild-type Se-supplemented mice. (**D**) Transgenic control mice. (**E**) Transgenic Se-deficient mice. (**F**) Transgenic Se-supplemented mice.

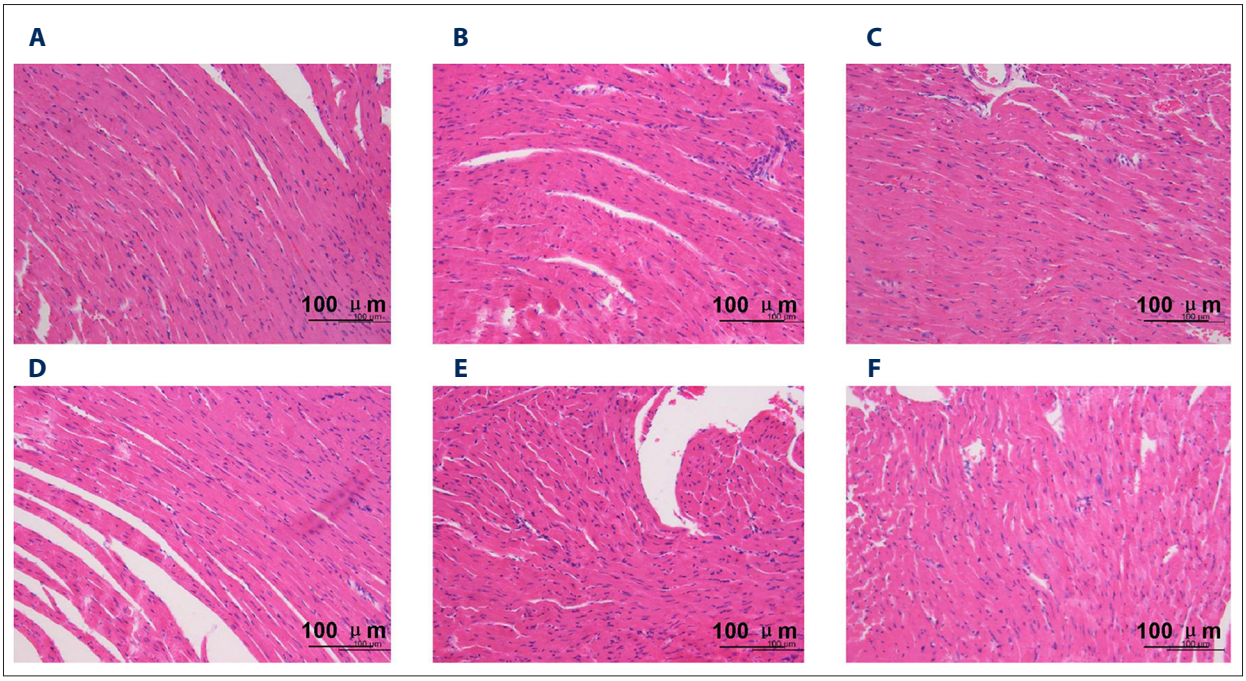

Figure 4. Myocardial HE staining of mice in each group. (**A**) Wild-type control mice. (**B**) Wild-type Se-deficient mice. (**C**) Wild-type Se-supplemented mice. (**D**) Transgenic control mice. (**E**) Transgenic Se-deficient mice. (**F**) Transgenic Se-supplemented mice. Scar bar=100 μm.

Indexed in: [Current Contents/Clinical Medicine] [SCI Expanded] [ISI Alerting System] [ISI Journals Master List] [Index Medicus/MEDLINE] [EMBASE/Excerpta Medica] [Chemical Abstracts/CAS]

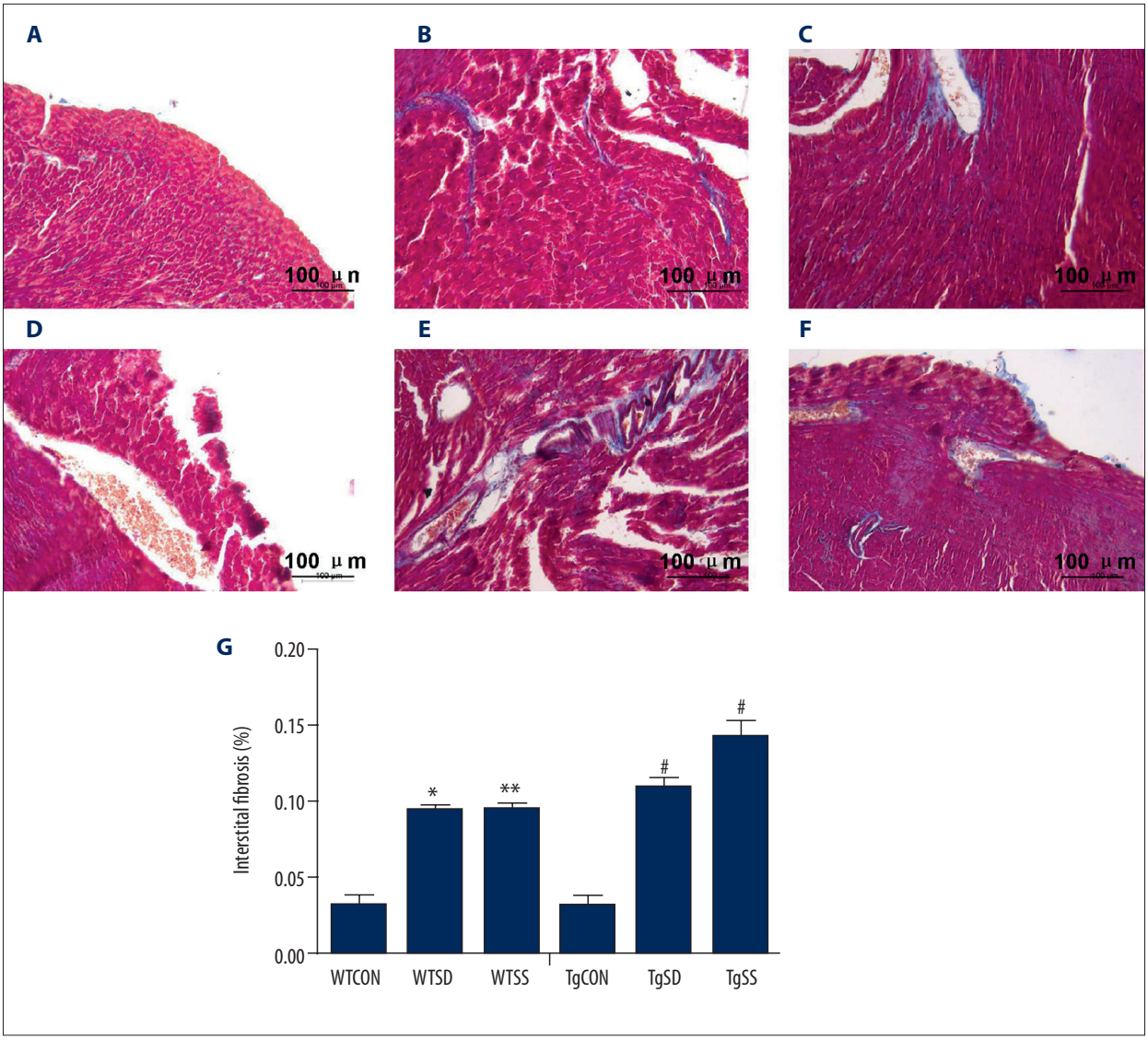

Figure 5. Masson's trichrome staining and statistical analysis of mice in each group. (**A**) Wild-type control mice. (**B**) Wild-type Se-deficient mice. (**C**) Wild-type Se-supplemented mice. (**D**) Transgenic control mice. (**E**) Transgenic Se-deficient mice. (**F**) Transgenic Se-supplemented mice. (**G**) Comparison of interstitial fibrosis of mice in each group. WTCON – wild-type control mice, WTSD – wild-type Se-deficient mice, WTSS – wild-type Se-supplemented mice, TgCON – transgenic control mice, TgSD – transgenic Se-deficient mice, TgSS – transgenic Se-supplemented mice. * $P<0.05$ *vs.* WTCON, ** $P<0.05$ *vs.* WTCON, TgSS, # $P<0.05$ *vs.* TgCON. Scar bar=100 μm.

fibrosis was not significantly different between WTSD and WTSS. In the Tg mice, myocardial fibrosis in SD and SS groups were also significantly increased compared with the CON group (Figure 5, $p<0.05$). Myocardial fibrosis was higher in TgSD but not significantly different from that in TgSS, while myocardial fibrosis in TgSS was significantly increased compared with that in the WTSS group (Figure 5, $p<0.05$).

Caspase-9 and caspase-3 expression levels

Caspase-9 in SD and SS groups was significantly higher than that in CON groups in WT mice and in Tg mice (Figure 6, $p<0.05$). Caspase-9 in WTSD was significantly increased compared with the WTSS group (Figure 6, $p<0.05$), while caspase-9 in TgSD was significantly lowered than that in WTSD group (Figure 6, $p<0.05$). Caspase-9 in TgSS was highly elevated over that in WTSS and TgSD groups (Figure 6, $p<0.05$).

Indexed in: [Current Contents/Clinical Medicine] [SCI Expanded] [ISI Alerting System] [ISI Journals Master List] [Index Medicus/MEDLINE] [EMBASE/Excerpta Medica] [Chemical Abstracts/CAS]

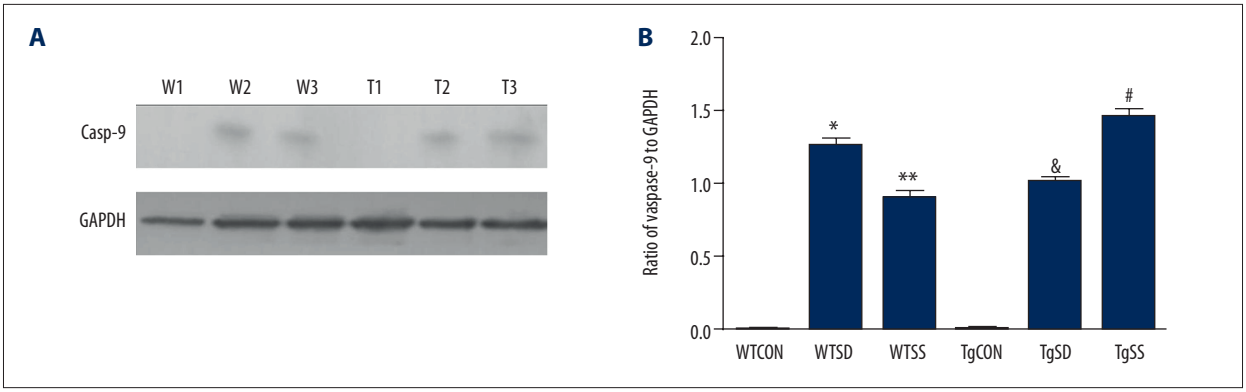

Figure 6. Expression level of caspase-9 in each group. (**A**) Image results of caspase-9. (**B**) Relative expression level of caspase-9. W1 – wild-type control mice, W2 – wild-type Se-deficient mice, W3 – wild-type Se-supplemented mice, T1 – transgenic control mice, T2 – transgenic Se-deficient mice, T3 – transgenic Se-supplemented mice. * $P<0.05$ *vs.* W1; ** $P<0.05$ *vs.* W1, W2, & $P<0.05$ *vs.* W2, T1; # $P<0.05$ *vs.* W3, T1, T2.

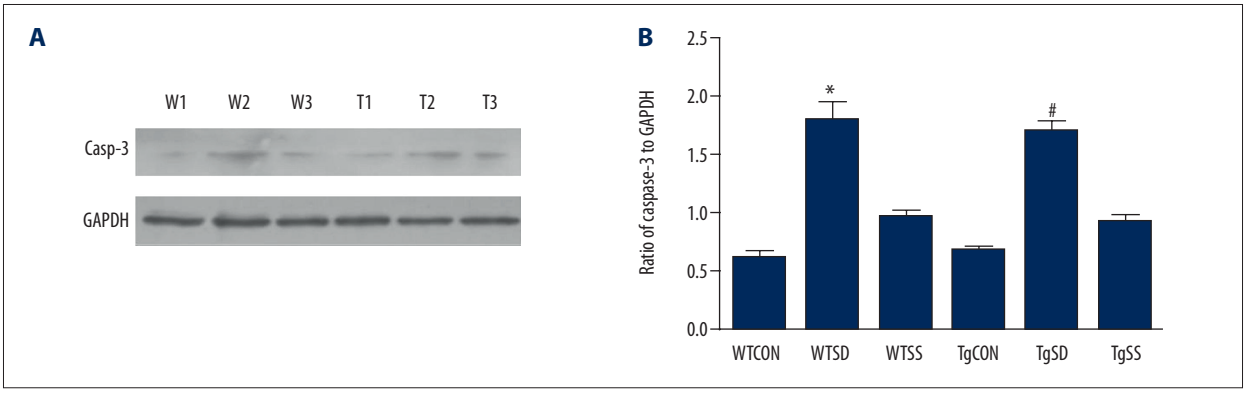

Figure 7. Expression level of caspase-3 in each group. (**A**) Image results of caspase-9. (**B**) Relative expression level of caspase-3. W1 – wild-type control mice, W2 – wild-type Se-deficient mice, W3 – wild-type Se-supplemented mice, T1 – transgenic control mice, T2 – transgenic Se-deficient mice, T3 – transgenic Se-supplemented mice. * $P<0.05$ *vs.* W1, W3, # $P<0.05$ *vs.* T1, T3.

Caspase-3 in the SD group was significantly increased over that in the CON group in WT mice and in Tg mice (Figure 7, $p<0.05$), and caspase-3 in SS groups was higher but was not significantly different from than that in the CON groups. Caspase-3 in TgSD and TgSS groups was slightly lowered compared with the respective WTSD and WTSS groups (Figure 7).

Discussion

It is well known that Se deficiency is associated with reversible heart failure that can be improved by Se supplementation [28–30]. Lei first found that the single-nucleotide polymorphism (Pro198Leu) in GPx-1 gene of KD patients is associated with Se deficiency as well as decreased GPx-1 activity. To further elucidate the hypothesis that both Se and the mutated GPx-1 gene might increase the risk of KD, the GPx-1P198L transgenic mice were generated and fed diets with different concentrations of Se. In the present study, Serum Se levels and cardiac GPx activity were remarkably decreased by Se deficiency in both WT and Tg mice. Serum Se levels in Se-supplemented groups were elevated but the difference was not significant, which was consistent with a previous study [9]. However, in WT mice, Se supplementation significantly increased GPx activity, which was even higher in Tg mice.

Our study provides evidence that overexpression of human GPx-1-198Leu does not exert protection against Se-deficiency-reduced cardiac remodeling and dysfunction. Cardiac systolic dysfunction was observed in Se-deficient mice and in Se-supplemented mice. The genotype did not work on improvement of cardiac function. As shown in Table 1 and Figure 3, the interventricular septum wall thickness in systole was significantly decreased in Se-deficient wild-type mice. Strangely, the ventricular posterior wall thickness was significantly increased in Se-supplemented transgenic mice. The left ventricle was heavily expanded, as evidenced by increased LVEDD and LVESD resulting from Se-deficient and Se-supplemented wild-type and transgenic mice, which indicates that the walls move poorly and the left ventricle diameter varies little from diastole

Indexed in: [Current Contents/Clinical Medicine] [SCI Expanded] [ISI Alerting System] [ISI Journals Master List] [Index Medicus/MEDLINE] [EMBASE/Excerpta Medica] [Chemical Abstracts/CAS]

to systole. Thus, cardiac systolic function was impaired by Se deficiency and Se supplement, not only in WT but also in Tg mice, which was also manifested as significantly lower EF and FS. Cardiac systolic dysfunction due to Se deficiency was not improved by overexpression of GPx-1-198Leu, which might be secondary to Ca2+ transport abnormalities of sarcoplasmic reticulum resulting from Se deficiency [31]. Unexpectedly, Se supplementation also led to systolic dysfunction. Metes-Kosik found that Se supplementation resulted in diastolic dysfunction [9]. Thus, we hypothesized that systolic dysfunction in Se-supplemented mice was secondary to chronic diastolic dysfunction. The elevated LVEDD and LVESD detected in Se-supplemented mice indicates that too much blood returned to the heart and the heart could not pump the increased blood volume into the systemic circulation; consequently, cardiac systolic dysfunction occurred.

Pathological changes in mice in different groups were detected to offer direct histomorphometry evidence for the above myocardial abnormalities. HE staining results showed that myocytes in Se-deficient mice became small with wave-like arrangement, gaps between cells were widened, and more inflammatory cells were observed. In Se-supplemented mice, myocytes were large with wave-like arrangement and crowded, and more inflammatory cells were also detected. Interstitial fibrosis was significantly increased due to Se deficiency and supplementation in WT and Tg mice. Fortunately, this provided us evidence that cardiac dysfunction was probably attributable to cardiac fibrosis and remodeling.

Lower Se level is associated with increased reactive oxygen species (ROS) production, a condition termed oxidative stress. Mitochondria are an important source of ROS within most mammalian cells [32–35]. Accumulated ROS in mitochondria can lead to oxidative damage to mitochondrial proteins, membranes, and DNA, impairing the metabolic functions of mitochondria and contributing to a variety of pathologies [36–39]. In addition, mitochondrial ROS also plays an important role in redox signaling from the organelle to the rest of the cell [40–42]. Mitochondrial oxidative damage can also increase the release of cytochrome c to the cytosol and thereby activate the cell apoptotic pathway. Se functions as an important antioxidant to detoxify ROS via selenoproteins, one of which is GPx-1, the major layer reducing lipid peroxides and hydrogen peroxide. Both Se deficiency and excess result in abnormal cellular defence mechanisms against oxidative stress [43,44]. Thus, in the present study, activation of caspase-9 and -3 were detected in Se-deficient WT mice. With no significant decrease in caspase-3, overexpression of GPx-1-198Leu gene in Se-deficient mice significantly attenuated the activation of caspase-9, which was still significantly higher than in control mice. Consistent with previous reports [44], Se supplementation in WT mice also led to increased caspase-9, which was much more highly elevated in Se-supplemented Tg mice. Caspase-3 in Se-supplemented mice was higher than in control animals but the difference was not significant, indicating that Se deficiency and supplementation can cause myocardial abnormalities via the mitochondria apoptotic pathway. Overexpression of GPx-1-198Leu did increase cardiac GPx activity and had some effects of inhibition to Se deficiency. However, the protection was not strong enough to exert significant improvement on cardiac structural and functional abnormalities. This provides evidence that the decreased activity of GPx-1-198Leu gene as well as Se deficiency might play a synergistic role in the pathogenesis of KD. High concentrations of Se may lead to assembly of the apoptotic molecules and ROS, which induce mitochondrial membrane permeabilization and caspase activation [5]. It has been reported that lipid peroxidation (LPO) was significantly increased in the liver of mice fed a 0.4-Se/kg diet compared to the animals fed a 0.1 Se/kg diet [45]. Since GPx-1 is considered to be the body storage form of Se and to serve a homeostatic function in Se metabolism [46], more Se might have been deposited in the Tg mice. In the presence of GSH, high concentrations of Se can react to become selenide anion (RSe-), hydrogen selenide (H2Se) [47], and GSSe- [1], which react with O2 or GSH and then more super-oxidative anion are produced, and finally the mitochondria apoptotic pathway is activated [1,44,47]. Decreases in activity of superoxide dismutase (SOD) have been reported both in Se-deficient and Se-excess diet-fed mice [48]. Thus, it is understandable that accumulated superoxide was not successfully detoxified in Se-deficient or in supplemented animals, although GPx activity in Se-supplemented animals was elevated.

Conclusions

We have demonstrated that both Se deficiency and supplementation induced myocardial structural and functional abnormalities via activation of caspase-9 and -3, but overexpression of human GPx-1-198Leu could not attenuate cardiac injuries caused by Se deficiency and Se supplementation. Blocking the mitochondrial apoptotic pathway might impede the occurrence and development of Se-related cardiomyopathy.

Conflict of interests

None.

Indexed in: [Current Contents/Clinical Medicine] [SCI Expanded] [ISI Alerting System] [ISI Journals Master List] [Index Medicus/MEDLINE] [EMBASE/Excerpta Medica] [Chemical Abstracts/CAS]

References:

1. Mertens K, Lowes DA, Webster NR et al: Low zinc and selenium concentrations in sepsis are associated with oxidative damage and inflammation. Br J Anaesth, 2015; 114: 990–99
2. Liu H, Li X, Qin F et al: Selenium suppresses oxidative stress-enhanced vascular smooth muscle cell calcification by inhibiting the activation of the PI3K/AKT and ERK signaling pathways and endoplastic reticulum stress. J Biol Inorg Chem, 2014; 19: 375–88
3. Week BS, Hanna MS, Cooperstein D: Dietary selenium and selenoprotein function. Med Sci Monit, 2012; 18: RA127–32
4. Misra S, Selvam AK, Wallenberg M et al: Selenite promotes all-trans retinoic acid-induced maturation of acute promyelocytic leukemia cells. Oncotarget, 2016; 7: 74686–700
5. Guan L, Han B, Li J et al: Exposure of human leukemia NB4 cells to increasing concentrations of selenite switches the signaling from pro-survival to pro-apoptosis. Ann Hematol, 2009; 88: 733–42
6. Jia C, Chen X, Li X et al: The effect of DHEA treatment on the oxidative stress and myocardial fibrosis induced by Keshan disease pathogenic factors. J Trace Mlem Med Biol, 2011; 25: 154–59
7. Metes-Kosik N, Luptak I, Dibello PM et al: Both selenium deficiency and modest selenium supplementation lead to myocardial fibrosis in mice via effects on redox-methylation balance. Mol Nutr Food Res, 2012; 56: 1812–24
8. Arroyo M, Laguardia SP, Bhattacharya SK et al: Micronutrients in African-Americans with decompensated and compensated heart failure. Transl Res, 2006; 148: 301–8
9. Metes-Kosik N, Luptak I, Dibello PM et al: Both selenium deficiency and modest selenium supplementation lead to myocardial fibrosis in mice via effects on redox-methylation balance. Mol Nutr Food Res, 2012; 56: 1812–24
10. Li H, Juan L, Xia L et al: Thioridazine sensitizes esophageal carcinoma cell lines to radiotherapy-induced apoptosis *in vitro* and *in vivo*. Med Sci Monit, 2016; 22: 2624–34
11. Carrasco E, Calvo MI, Blazquez-Castro A et al: Photoactivation of ROS production *in situ* transiently activates cell proliferation in mouse skin and in the hair follicle stem cell niche promoting hair growth and wound healing. J Invest Dermatol, 2015; 135: 2611–22
12. Sun A, Lin J, Pi C et al: Biological evaluation of ferrocenyl olefins: Cancer cell growth inhibition, ROS production, and apoptosis activity. Arch Pharm (Weinheim), 2016; 349: 186–92
13. Gupta RK, Patel AK, Shah N et al: Oxidative stress and antioxidants in disease and cancer: A review. Asian Pac J Cancer Prev, 2014; 15: 4405–9
14. Bhat AH, Dar KB, Aness S et al: Oxidative stress, mitochondrial dysfunction and neurodegenerative diseases: A mechanistic insight. Biomed Pharmacother, 2015; 74: 101–10
15. Santilli F, Guagnano MT, Vazzana N et al: Oxidative stress drives and modulators in obesity and cardiovascular disease: From biomarkers to therapeutic approach. Curr Med Chem, 2015; 22: 582–95
16. Lei C, Niu X, Wei J et al: Interaction of glutathione peroxidase-1 and selenium in endemic dilated cardiomyopathy. Clin Chim Acta, 2009; 399: 102–8
17. Miller JC, Thomson CD, Williams SM et al: Influence of the glutathione peroxidase 1 Pro200Leu polymorphism on the response of glutathione peroxidase activity to selenium supplementation: A randomized controlled trial. Am J Clin Nutr, 2012; 96: 923–31
18. Blein S, Berndt S, Joshi AD et al: Factors associated with oxidative stress and cancer risk in the breast and prostate cancer cohort consortium. Free Radic Res, 2014; 48: 380–86
19. Spisak K, Klimkowicz-Mrowiec A, Pera J et al: rs2070421 of the SOD1 gene is associated with risk of Alzheimer's disease. Neurol Neurochir Pol, 2014; 48: 342–45
20. Seara FAC, Maciel L, Barbosa RAQ et al: Cardiac ischemia/reperfusion injury is inversely affected by thyroid hormones excess or deficiency in male wistar rats. PLoS One, 2018; 13: e0190355
21. Takenaka H, Kihara Y, Iwanaga Y et al: Angiotensin II, oxidative stress, and extracellular matrix degradation during transition to LV failure in rats with hypertension. J Mol Cell Cardiol, 2006; 41: 989–97
22. Wiedenmann T, Dietrich N, Fleming T et al: Modulation of glutathione peroxidase activity by age-dependent carbonylation in glomeruli of diabetic mice. J Diabetes Complications, 2018; 32: 130–38
23. Merry TL, Tran M, Dodd GT et al: Hepatocyte glutathione peroxidase-1 deficiency improves hepatic glucose metabolism and decreases steatohepatitis in mice. Diabetologia, 2016; 59: 2632–44
24. Yu Y, Song J, Guo X et al: Characterization and structural analysis of human selenium-dependent glutathione peroxidase 4 mutant expressed in *Escherichia coli*. Free Radic Biol Med, 2014; 71: 332–38
25. Liu ZW, Niu XL, Chen KL et al: Selenium attenuates adriamycin-induced cardiac dysfunction via restoring expression of ATP-sensitive potassium channels in rats. Biol Trace Elem Res, 2013; 153: 220–28
26. Kume H, Okazaki K, Yamaji T et al: A newly designed enteral formula containing whey peptides and fermented milk product protects mice against concanavalin A-induced hepatitis by suppressing overproduction of inflammatory cytokines. Clin Nutr, 2012; 31: 283–89
27. Roe ND, Ren J: Oxidative activation of Ca(2+)/calmodulin-activated kinase II mediates ER stress-induced cardiac dysfunction and apoptosis. Am J Physiol Heart Circ Physiol, 2013; 304: H828–39
28. Yang J, Wang T, Wu C et al: Selenium level surveillance for the year 2007 of Keshan disease in endemic areas and analysis on surveillance results between 2003 and 2007. Biol Trace Elem Res, 2010; 138: 53–59
29. Al-Matary A, Hussain M, Ali J: Selenium: A brief review and a case report of selenium responsive cardiomyopathy. BMC Pediatr, 2013; 13: 39
30. Boldery R, Fielding G, Rafter T et al: Nutritional deficiency of selenium secondary to weight loss (bariatric) surgery associated with life-threatening cardiomyopathy. Heart Lung Circ, 2007; 16: 123–26
31. Swedberg K: Heart failure therapies in 2014: Mixed results for heart failure therapies. Nat Rev Cardiol, 2015; 12: 73–75
32. Shabalina IG, Vrbacky M, Pecinova A et al: ROS production in brown adipose tissue mitochondria: the question of UCP1-dependence. Biochim Biophys Acta, 2014; 1837: 2017–30
33. Oyewole AO, Birch-Machin MA: Mitochondria-targeted antioxidants. FASEB J, 2015; 29: 4766–71
34. Mracek T, Holzerova E, Drahota Z et al: ROS generation and multiple forms of mammalian mitochondrial glycerol-3-phosphate dehydrogenase. Biochim Biophys Acta, 2014; 1837: 98–111
35. Yang Y, Karakhanova S, Hartwig W et al: Mitochondria and mitochondrial ROS in cancer: Novel targets for anticancer therapy. J Cell Physiol, 2016; 231: 2570–81
36. Scott TL, Rangaswamy S, Wicker CA et al: Repair of oxidative DNA damage and cancer: Recent progress in DNA base excision repair. Antioxid Redox Signal, 2014; 20: 708–26
37. Davidson SM, Duchen MR: Endothelial mitochondria: Contributing to vascular function and disease. Circ Res, 2007; 100: 1128–41
38. Suzuki M, Bandoski C, Bartlett JD: Fluoride induces oxidative damage and SIRT1/autophagy through ROS-mediated JNK signaling. Free Radic Biol Med, 2015; 89: 369–78
39. Borodkina A, Shatrova A, Abushik P et al: Interaction between ROS dependent DNA damage, mitochondria and p38 MAPK underlies senescence of human adult stem cells. Aging (Albany, NY), 2014; 6: 481–95
40. Suzuki N, Koussevitzky S, Mittler R et al: ROS and redox signalling in the response plants to abiotic stress. Plant Cell Environ, 2012; 35: 259–70
41. Ozgur R, Turkan I, Uzilday B et al: Endoplasmic reticulum stress triggers ROS signalling, changes the redox state, and regulates the antioxidant defence of Arabidopsis thaliana. J Exp Bot, 2014; 65: 1377–90
42. Yang Y, Song Y, Loscalzo J: Regulation of the protein disulfide proteome by mitochondria in mammalian cells. Proc Natl Acad Sci USA, 2007; 104: 10813–17
43. Koszta G, Fulesdi B: Significance of selenium in the pathogenesis and therapy of cardiovascular diseases and those requiring intensive care. Orv Hetil, 2013; 154: 1621–27
44. Liu CP, Fu J, Xu FP et al: The role of heat shock proteins in oxidative stress damage induced by Se deficiency in chicken livers. Biometals, 2015; 28: 163–73
45. Kang BP, Bansal MP, Mehta U: Hyperlipidemia and type I 5'-monodeiodinase activity: Regulation by selenium supplementation in rabbits. Biol Trace Elem Res, 2000; 77: 231–39
46. King N, Lin H, Suleiman MS: Cysteine protects freshly isolated cardiomyocytes against oxidative stress by stimulating glutathione peroxidase. Mol Cell Biochem, 2010; 343: 125–32

Indexed in: [Current Contents/Clinical Medicine] [SCI Expanded] [ISI Alerting System] [ISI Journals Master List] [Index Medicus/MEDLINE] [EMBASE/Excerpta Medica] [Chemical Abstracts/CAS]

47. Spallholz JE, Palace VP, Reid TW: Methioninase and selenomethionine but not Se-methylselenocysteine generate methylselenol and superoxide in an *in vitro* chemiluminescent assay: Implications for the nutritional carcinostatic activity of selenoamino acids. Biochem Pharmacol, 2004; 67: 547–54

48. Qin S, Huang B, Ma J et al: Effects of selenium-chitosan on blood selenium concentration, antioxidation status, and cellular and humoral immunity in mice. Biol Trace Elem Res, 2015; 165: 145–52

Indexed in: [Current Contents/Clinical Medicine] [SCI Expanded] [ISI Alerting System] [ISI Journals Master List] [Index Medicus/MEDLINE] [EMBASE/Excerpta Medica] [Chemical Abstracts/CAS]